

Open charm production at RHIC

Xin Dong^a

^aDepartment of Modern Physics, University of Science and Technology of China - USTC, 96 Jinzhai Road, Hefei, Anhui 230026, China

Recent experimental measurements on open charm production in proton-proton, proton (deuteron)-nucleus and nucleus-nucleus collisions at RHIC are reviewed. A comparison with theoretical predictions is made. Some unsettled issues in open charm production call for precise measurements on directly reconstructed open charm hadrons.

1. Introduction

The ongoing four experiments at the Relativistic Heavy Ion Collider (RHIC) are designed to search for and measure the quark-gluon plasma (QGP), a new state of matter composed of deconfined, locally thermalized quarks and gluons. The equilibrated matter is expected to be described by the equation of state (EoS) with partonic degrees of freedom. The partonic pressure gradient and the temperature are two important characteristics within such kind of EoS.

The physics results from the first three-year runs at RHIC demonstrate that the partonic pressure gradient has been developed during the system evolution in heavy ion collisions. This has been illustrated in the “white papers” from four experiments [1]. To determine the partonic EoS, the next task is to test the local and early thermalization hypothesis *experimentally*. Heavy quark (c, b) is an ideal probe to this end. Due to its much heavier mass, it requires more rescatterings to reach the comparable collectivity as light quark (u, d, s). If heavy quark collectivity is observed, there must be even more rescatterings happening among light quarks than expected, because the rescattering cross section among light quarks is larger than that between heavy and light quarks. So heavy quark collectivity can be used as an indicator for the thermalization of light flavors, although heavy quarks themselves do not have to be thermalized [2].

Since charm quark creation requires a large momentum transfer *i.e.* $Q \gtrsim 3$ GeV, it is believed to be less affected by non-perturbative effects in pQCD calculations. So the measurement on charm quark production in proton-proton ($p + p$) collisions not only provides a necessary reference for heavy ion collisions, but also enables us to test the pQCD calculations on both total and differential cross sections.

In heavy ion collisions, the theoretical calculation shows that charm quarks are mostly created through initial gluon-gluon fusions [3]. And since charm quark mass is much larger than the estimated system temperature, its production is little influenced by the thermal component. Unlike light quark, heavy quark mass is dominated by its current quark mass - the mass originating from the coupling with the electroweak Higgs field [4]. Therefore

heavy quark is an ideal penetrating probe to the rescatterings and thermalization at the early stage of heavy ion collisions.

The radiative energy loss of charm quark in vacuum is characterized by the ‘‘dead-cone’’ effect [5]. When an energetic charm quark traverses through the dense medium, it will interact with surrounding partons. Theoretical calculations predict that the suppression of the nuclear modification factor (R_{AA}) for charm quarks in central nucleus-nucleus ($A + A$) collisions is smaller than that of light quarks [6–8]. Most of these predictions were made based on the radiative energy loss mechanism and the medium properties to our knowledge (gluon density *etc.*). The interaction between charm quark with medium can also be reflected by the charm quark elliptic flow (v_2). The coalescence approach in a thermalized medium shows that charm hadrons may obtain a finite v_2 even if charm quarks have a zero v_2 [9]. The charm quark collectivity has been studied in an AMPT transport model, and the result shows that a large charm quark interacting cross section is needed to produce the magnitude of v_2 comparable with that of light quarks [10]. Measurements of the charm quark collectivity will tell us the degree to which charm quarks interact with other partons, and then provide us with pivotal information on the early thermalization of light flavors.

PHENIX and STAR experiments at RHIC have the capability to detect charms. PHENIX measures open charms through their semi-leptonic decays: electrons in central arms in mid-rapidity and muons in muon arms in forward/backward rapidities. STAR can reconstruct open charm mesons through their hadronic decays in the TPC. It can also identify electrons with the help of other sub-detectors [11,12]. The advantage of PHENIX is that it has low budget materials in its inner detectors, while STAR has a large acceptance in the TPC around the mid-rapidity.

2. Charm production in elementary $p + p$ and $d + A$ collisions

The first reconstruction of open charm hadrons through their hadronic decays was reported by the STAR Collaboration in the last Quark Matter conference [11] and was recently published in Ref. [12]. The reconstructed charm hadrons and decay channels in $d + Au$ collisions are $D^0 \rightarrow K^- \pi^+$, $D^{*+} \rightarrow D^0 \pi^+$ and their charge conjugate channels. The p_T coverage is $p_T < 3$ GeV/ c for D^0 and $1 < p_T/(\text{GeV}/c) < 6$ for D^{*+} respectively. Event mixing technique was used to construct the combinatorial background in the invariant mass spectrum.

STAR also reported the results of non-photonic electrons mostly from heavy flavor decays [11,12]. Results from independent analysis using three different electron identification methods (rdE/dx , $dE/dx+\text{TOF}$, $dE/dx+\text{EMC}$) are in good agreement in both $p + p$ and $d + Au$ collisions. The non-photonic electron spectrum is also consistent with that deduced from STAR’s data for open charm mesons. The combined fit of the total charm cross section for D^0 and non-photonic electrons is $\sigma_{c\bar{c}}^{NN} = 1.4 \pm 0.2 \pm 0.4$ mb at $\sqrt{s_{NN}} = 200$ GeV [12]. Within errors, the electron spectra in $p + p$ and $d + Au$ collisions show approximate N_{bin} scaling, implying no significant nuclear effect in $d + Au$ collisions.

PHENIX reported its spectra of the non-photonic electrons from charm hadron decays via three independent methods: the cocktail, the convertor, and the $\gamma - e$ correlation [13, 14]. These methods all give a consistent result: $\sigma_{c\bar{c}}^{NN} = 0.92 \pm 0.15 \pm 0.54$ mb in $p + p$

collisions compatible with the STAR data. Measurements of centrality dependence of non-photonic electrons in $d + \text{Au}$ collisions also shows the N_{bin} scaling [13].

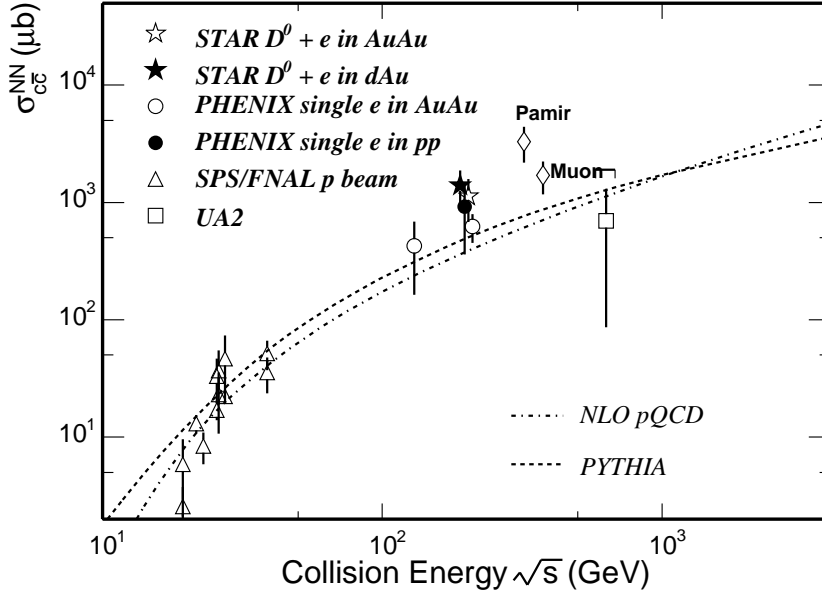


Figure 1. The total $c\bar{c}$ cross section per nucleon-nucleon collision vs. the collision energies. The low energy data points are selected from fixed target experiments [15,16]. The diamonds depict two cosmic ray measurements [17]. The dashed and dot-dashed lines are taken from [12].

Available data for the cross production cross section at various energies are shown in Fig. 1. The results in Au + Au collisions at RHIC will be discussed in the next section. The dot-dashed curve depicts a typical next-to-leading (NLO) pQCD calculation where parameters are optimized to fit the low energy data [18]. The dashed curve is a PYTHIA (version 6.152) simulation with the parton distribution function CTEQ5M1. Both the NLO pQCD calculation and the PYTHIA prediction give a total cross section of 300 – 450 μb , 2 – 3 times lower than the experimental data. Data points from cosmic ray experiments also support a large cross section at $\sqrt{s} \sim 300$ GeV [17]. Recent analysis of open beauty measurements by CDF shows high order processes (*e.g.* initial/final radiation, gluon splitting, and parton shower production) contribute to a large part in heavy flavor production at Tevatron [19]. The discrepancy at RHIC energy between data and predictions indicates that these processes may play more important role in theoretical model than previous thought.

Apart from an overall normalization factor, the electron spectral shapes measured by PHENIX and STAR are consistent with each other within errors. Shown in Fig. 2, the measured spectra are clearly harder than the overall contribution from charm and bottom decays in the PYTHIA simulation. An important issue in obtaining the charm production

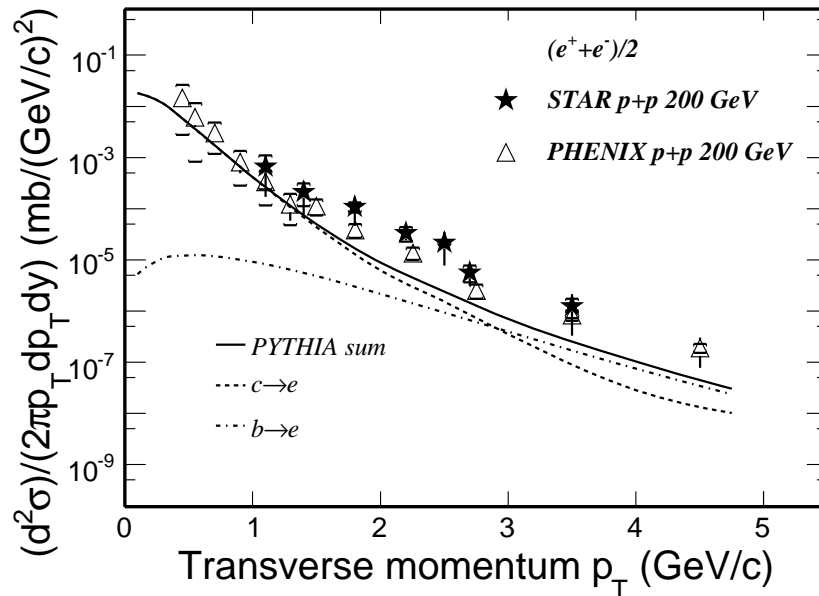


Figure 2. Non-photonic electron spectrum in $p + p$ collisions compared with PYTHIA model LO calculation. The data points are taken from [12] and [14]. The PYTHIA model parameter setting is inspired by the publication for Au + Au 130 GeV data [20] with $\sigma_{c\bar{c}} = 658 \mu\text{b}$.

in the electron approach is how to determine the bottom contamination. A recent NLO pQCD investigation at RHIC energy tells us that the crossing point between the electron spectra from charm decays and bottom decays may vary in a broad p_T range ($\sim 3 - 10$ GeV/c) [21]. This will bring very large uncertainties in electron data from bottom decays.

The reconstructed D^0 spectrum covers more than 90% of the total charm yields, while the electron spectrum at $p_T > 0.8$ GeV/c only covers $\sim 15\%$. To establish a good reference for studying charm production in heavy ion collisions, precise measurements on reconstructed charm hadron with large p_T coverage are necessary.

3. Open charm production in A + A collisions

3.1. Charm yields

Charm yields in heavy ion collisions are expected to be scaled by N_{bin} since most charm quark pairs are created in the initial hard scatterings. A recent publication from the PHENIX Collaboration reported the centrality dependence of non-photonic electron spectra in Au + Au collisions at $\sqrt{s_{NN}} = 200$ GeV [22]. The electron spectra in all centrality bins show approximate N_{bin} scaling with respect to $p+p$ collisions. The obtained charm total cross section in minimum bias Au + Au collisions is $0.622 \pm 0.057 \pm 0.160$ mb, compatible with the that in $p + p$ collisions.

At this conference STAR reported reconstructed D^0 signals in minimum bias Au + Au collisions using the same method as that in $d + Au$ collisions [23]. They also reported

centrality dependence of non-photonic electron measurements in Au + Au collisions [23, 24]. By combining D^0 and non-photonic electrons, the extracted total charm cross section per nucleon-nucleon collision in minimum bias Au + Au collisions is $\sigma_{c\bar{c}}^{NN} = 1.13 \pm 0.09 \pm 0.42$ mb, consistent with the STAR $d + Au$ result and the PHENIX $p + p$ result. The cross section results from Au + Au collisions, measured by PHENIX and STAR, are illustrated in Fig. 1.

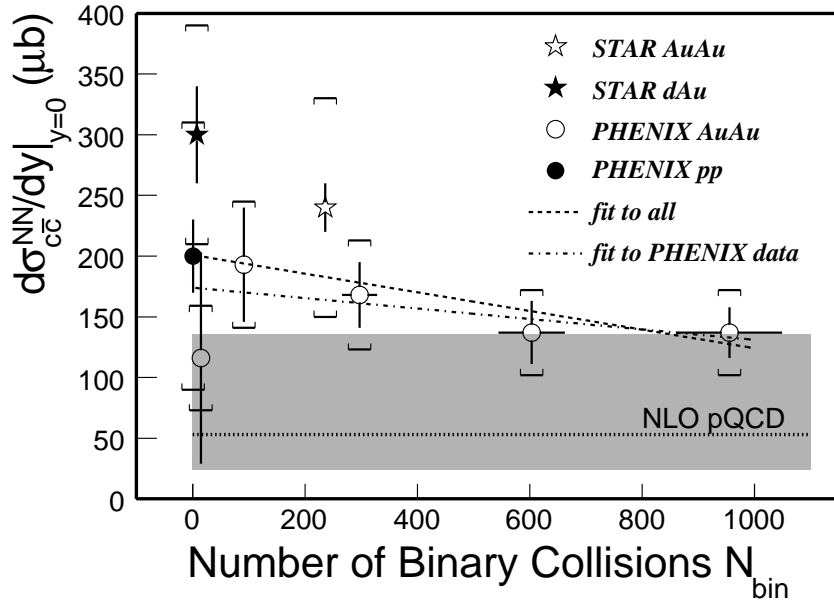


Figure 3. A summary of measurements of the differential $c\bar{c}$ cross section at mid-rapidity per nucleon-nucleon collision vs. the number of binary collisions at $\sqrt{s_{NN}} = 200$ GeV. The dotted line together with the grey band depict a typical NLO pQCD calculation with uncertainties from Ref. [21]. The dashed and dot-dashed lines are linear fits to all data and PHENIX data respectively.

A summary of available data on charm cross sections at 200 GeV is given in Fig. 3. All measurements agree with each other within large error bars. The dotted line together with the grey band display a typical NLO pQCD calculation with uncertainties [21]. N_{bin} scaling is assumed in the extrapolation from $p + p$ to $d + Au$ and to Au + Au collisions. The data are systematically above this band. One sees from data that there is a slightly decrease from $p + p$ ($d + Au$) to peripheral Au + Au, and then to central Au + Au collisions, as shown by the dashed and dot-dashed lines which fit to all data and PHENIX ones respectively. But we cannot claim much due to large errors.

The total cross section measurements are important references for charmonium production whose enhancement or suppression in central Au + Au collisions is thought to be a robust signal of the QGP. More precise charm measurements in various centralities in Au + Au collisions are needed.

One interesting observation, described in Ref. [25], is that the centrality dependence of charm yields can be explained marginally by the differential cross section of inclusive hadrons integrated over $p_T > 1.5 \text{ GeV}/c \sim m_D$. This means the production of a variety of particles is not sensitive to the flavor quantity once the momentum transfer is above the threshold.

3.2. Charm quark energy loss in medium

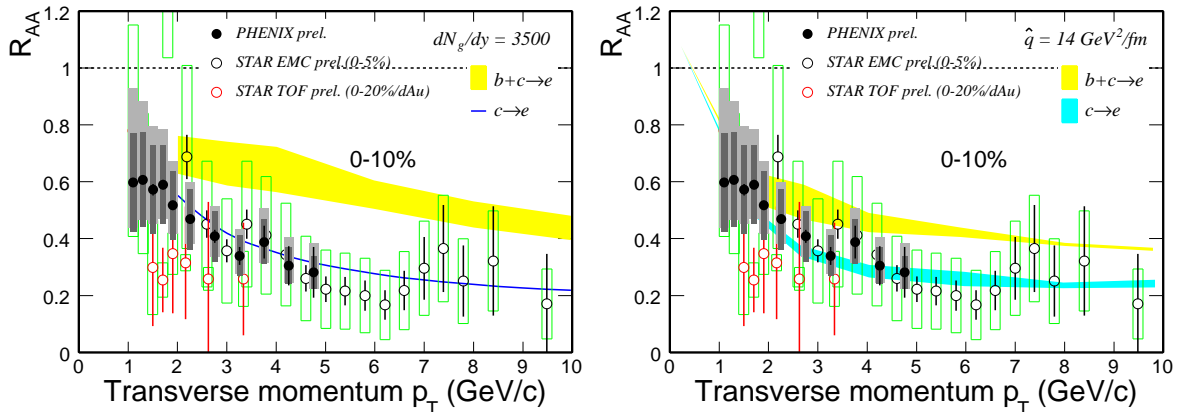


Figure 4. Recent measurements on non-photonic electron R_{AA} in central Au + Au collisions from PHENIX (top 0-10%) and STAR (top 0-5% from EMC and top 0-20% using d+Au as the reference from TOF) experiments compared with theoretical predictions (top 0-10%) from [27] (left plot) and [28] (right plot).

Given in Fig. 4 are recent results of the nuclear modification factor R_{AA} of non-photonic electrons in central Au + Au collisions from PHENIX [26] and STAR [23,24]. The data give a consistent, and *surprising* fact: the suppression factor for non-photonic electrons is $\sim 0.2 - 0.3$, which is almost at the same level as that of charged hadrons in the similar p_T range. Two recent pQCD estimations in the radiative energy loss scenario are also shown in that figure [27,28]. These approaches try to fix the transport parameter (dN_g/dy or \hat{q}) boundaries by fitting to the R_{AA} for light hadrons. The boundaries obtained are $1000 < dN_g/dy < 3500$ and $4 < \hat{q}/(\text{GeV}^2/\text{fm}) < 14$ respectively. One sees in Fig. 4 the upper limit to which energetic partons lose the largest fraction of their energies in the medium due to gluon bremsstrahlung from these two approaches. The comparison with the data illustrates the suppression of electrons from charm decays may reach as low as that of light hadrons. However, if the bottom contribution is included according to pQCD calculations, the overall electron R_{AA} will increase to $\sim 0.4 - 0.5$. This is a significant discrepancy compared to the data at $4 < p_T/(\text{GeV}/c) < 7$. If the data in Fig. 4 are confirmed to be correct, this will bring at least two open issues: (i) if the current radiative energy loss mechanism persists, there is no much room for the bottom's contribution in the non-photonic electron spectrum up to $p_T \sim 7 \text{ GeV}/c$. (ii) if the bottom's contribution is as what is given by the generic pQCD predictions (the crossing

point is $\sim 3 - 5 \text{ GeV}/c$), there must be other energy loss effects besides gluon radiation. These are challenges to theorists.

In several recent publications, some authors argued that because in momentum coverage $\gamma v \sim 1$, heavy quark is not ultrarelativistic, elastic collisional energy loss may play an important role when charm quarks traverse the medium [29,30]. They computed the R_{AA} in the hydrodynamic transport scenario, which gives the strong suppression as observed. The approach sheds light on the solution to the present discrepancy. To decouple the above two issues, one should precisely measure reconstructed open charm hadrons instead of electrons. Certainly, a precise reference in $p + p$ collisions on reconstructed open charm hadrons is needed.

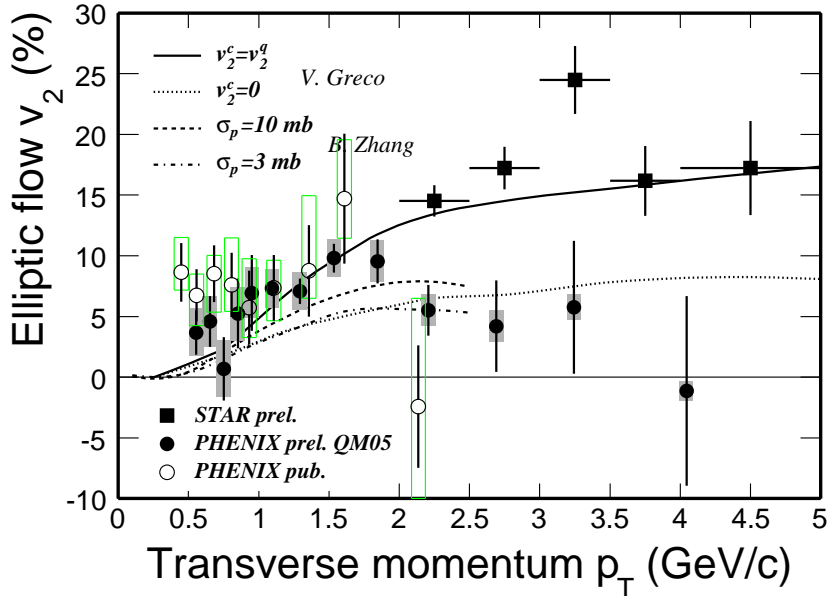


Figure 5. Recent measurements of v_2 for non-photonic electron in minimum bias Au + Au collisions from PHENIX [26,31] and STAR [32] and the comparison with theoretical predictions in [9,10]

3.3. Charm quark elliptic flow

PHENIX and STAR recently measured v_2 for non-photonic electrons in minimum bias Au + Au collisions [26,31,32], see Fig. 5. At $p_T > 2 \text{ GeV}/c$, even with the claimed $\sim 20 - 30\%$ systematic error by STAR, the measurements are not quite consistent between two experiments. In terms of the magnitude, v_2 for non-photonic electrons is comparable to that of other hadrons [33] in $p_T < 2 \text{ GeV}/c$. Two model predictions are also shown in that figure. Since there is an inconsistency between two experiments and the bottom's contribution is uncertain at $p_T > 2 \text{ GeV}/c$, let us focus on the range at $p_T < 2 \text{ GeV}/c$. In the coalescence model for a thermalized system [9], the picture that charm quark v_2 is the same as light quark v_2 is supported by the data. Compared with the transport model

results [10], the data favors charm quark has a large rescattering cross section, indicating that the charm quark has a finite v_2 . Although it is hard to extract v_2 of charm hadrons from electron v_2 , the data suggest there can be a non-zero v_2 for the charm quark. If the non-zero charm quark collectivity is confirmed, it means light flavor thermalization at RHIC, as I have argued in the introduction section.

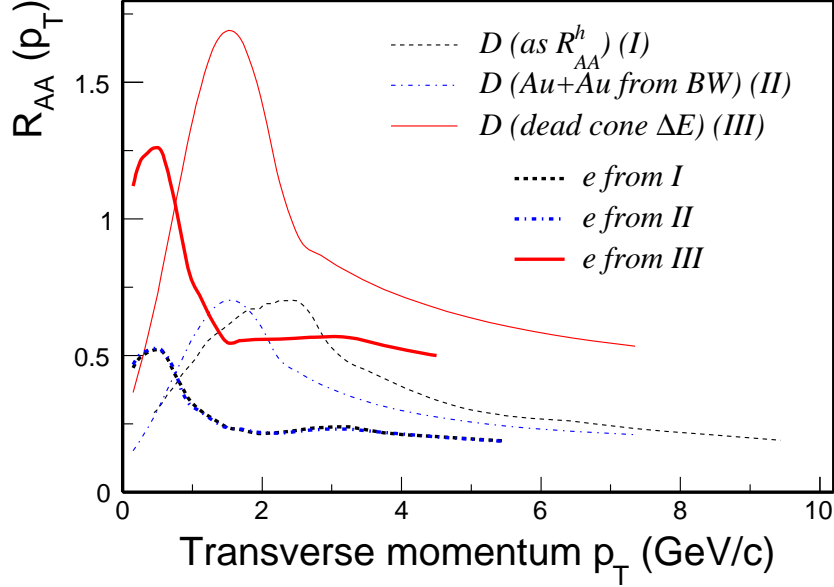


Figure 6. R_{AA} of charm hadrons (thin lines) and decayed electrons (thick lines) for several assumed D spectra in central Au + Au collisions. The charm hadron spectrum reference used in $p + p$ collisions is from STAR's $d + Au$ measurements [11]. The thin dashed line depicts the R_{AA} of charm hadrons same as that of charged hadrons. The thin dot-dashed line is for charm hadrons with the Blast-Wave (BW) behavior at $T_{fo} = 160$ MeV and $\langle\beta_T\rangle = 0.4c$ in low p_T and with the same behavior as charged hadrons' R_{AA} in high p_T [1]. The thin solid line is for D with the same BW parameters as the dot-dashed line in low p_T , but the total yield of charm hadrons is assumed to obey N_{bin} scaling. While in high p_T , their R_{AA} is taken from the dead-cone energy loss calculation in Ref. [6]. Thick lines depict the R_{AA} of electrons from charm decays with the distribution of the same line style.

3.4. Complementary remarks

From the measurements of R_{AA} and v_2 for other particles, the radiative energy loss can contribute to part of v_2 , but not much. In the recent work mentioned above [29], elastic collisions may provide a large fraction of energy loss of heavy quarks when $\gamma v \sim 1$. During hydrodynamical evolution, the flow of underlying medium will influence the heavy quark spectrum and heavy quark will pick up some flow. In this case, R_{AA} and v_2 are quite correlated, which means charm quark R_{AA} must be strong suppressed if a large v_2

is observed. So the combination of measurements on the charm quark spectrum and v_2 is essential, especially in low p_T region. The above arguments are based on the hydro assumptions.

To test the medium response to heavy quarks, the low p_T part is quite relevant. However, the electron spectrum from charm decays cannot disentangle different shapes in this p_T region due to smearing of the decay kinematics [34]. This effect can also be reflected on the R_{AA} of non-photonic electrons [16]. The simulation results of various input charm hadron's R_{AA} (thin curves) and the corresponding R_{AA} for electrons from charm decays (thick curves) are shown in Fig. 6. One sees that although at high p_T , the electron R_{AA} can reflect the suppression of charm hadrons (solid curves and dashed curves), the electron R_{AA} at low p_T cannot tell different thermal shapes (dashed curves and dot-dashed curves): the thick dashed and thick dot-dashed curves are almost identical. Therefore we need in the future precise measurements of the spectrum for reconstructed open charm hadrons at low p_T .

4. Conclusion and outlook

The heavy flavor program has started at RHIC extensively. Heavy flavor collectivity is expected to be an ideal probe to the light flavor thermalization. Plenty of new and surprising results on open charm production have been presented on this conference. However, most of present measurements use electrons decayed from charm hadrons which brings large uncertainties. The electron approach can be only a placeholder. We need precise measurements for reconstructed charm hadron spectra and v_2 in a wide p_T range. So the current sub-detector upgrade proposals in pipe for PHENIX and STAR detectors are very important to this goal [35–37]. With the upgraded inner tracking detector, PHENIX and STAR can reconstruct the secondary vertices of open charm decays with much lower background. We look forward to more exciting physical results from RHIC with upgraded detectors in the future.

5. Acknowledgement

I would like to thank the conference organizers for inviting me to present the talk. I appreciate many constructive discussions with M. Djordjevic, L. Grandchamp, M. Gyulassy, H. Huang, J. Raufeisen, H.-G. Ritter, K. Schweda, P. Sorensen, A. Tai, R. Vogt, Q. Wang, X.-N. Wang, N. Xu, Z. Xu and H. Zhang. This work is partially supported by the National Natural Science Foundation of China under the Grant No. 10475071.

REFERENCES

1. I. Arsene *et al.* (BRAHMS Collaboration), Nucl. Phys. A 757 (2005) 1; B.B. Back *et al.* (PHOBOS Collaboration), Nucl. Phys. A 757 (2005) 28; J. Adams *et al.* (STAR Collaboration), Nucl. Phys. A 757 (2005) 102; S.S. Adler *et al.* (PHENIX Collaboration), Nucl. Phys. A 757 (2005) 184.
2. X. Dong *et al.*, Phys. Lett. B 597 (2004) 328.
3. Z. Lin and M. Gyulassy, Phys. Rev. Lett. 77 (1996) 1222.
4. B. Müller, nucl-th/0404015.

5. Y. Dokshitzer and D. Kharzeev, Phys. Lett. B 519 (2001) 199.
6. M. Djordjevic, M. Gyulassy and S. Wicks, Phys. Rev. Lett. 94 (2005) 112301.
7. B.W. Zhang, E.K. Wang, X-N. Wang, Phys. Rev. Lett. 93 (2004) 072301.
8. N. Armesto *et al.*, Phys. Rev. D 71 (2005) 054027.
9. V. Greco, C.M. Ko and R. Rapp, Phys. Lett. B 595 (2004) 202.
10. B. Zhang, L.W. Chen, and C.M. Ko, nucl-th/0502056; B. Zhang *these proceedings*.
11. L. Ruan *et al.* (STAR Collaboration), J. Phys. G 30 (2004) S1197; A. Tai *et al.* (STAR Collaboration), J. Phys. G 30 (2004) S809; A.A.P. Suaide *et al.* (STAR Collaboration), J. Phys. G 30 (2004) S1179.
12. J. Adams *et al.* (STAR Collaboration), Phys. Rev. Lett. 94 (2005) 062301.
13. Y. Kwon *et al.* (PHENIX Collaboration), *these proceedings*.
14. S.S. Adler *et al.* (PHENIX Collaboration), nucl-ex/0508034.
15. S.P.K. Tavernier, Rep. Prog. Phys. 50 (1987) 1439, and references therein.
16. X. Dong, nucl-ex/0509011. Ph.D. Thesis, University of Science and Technology of China, 2005.
17. I.V. Rakobolskaya *et al.*, Nucl. Phys. B 112 (2003) 353c.
18. R. Vogt, Int. J. Mod. Phys. E 12 (2003) 211.
19. P.J. Bussey *et al.* (CDF Collaboration), hep-ex/0408020.
20. K. Adcox *et al.* (PHENIX Collaboration), Phys. Rev. Lett. 88 (2002) 192302.
21. M. Cacciari, P. Nason and R. Vogt, hep-ph/0502203; R. Vogt, *these proceedings*.
22. S.S. Adler *et al.* (PHENIX Collaboration), Phys. Rev. Lett. 94 (2005) 082301.
23. H. Zhang *et al.* (STAR Collaboration), *these proceedings*.
24. J. Bielcik *et al.* (STAR Collaboration), *these proceedings*.
25. Z. Xu, nucl-th/0410005.
26. S.A. Butsyk *et al.* (PHENIX Collaboration), *these proceedings*.
27. M. Djordjevic *et al.*, nucl-th/0507019; M. Djordjevic, *these proceedings*.
28. N. Armesto, *these proceedings*.
29. G.D. Moore and D. Teaney, Phys. Rev. C 71 (2005) 064904; D. Teaney, *these proceedings*.
30. H. van Hees, V. Greco and R. Rapp, nucl-th/0508055; R. Rapp, *these proceedings*.
31. S.S. Adler *et al.* (PHENIX Collaboration), Phys. Rev. C 72 (2005) 024901.
32. F. Laue *et al.* (STAR Collaboration), *these proceedings*.
33. M. Oldenberg *et al.* (STAR Collaboration), *these proceedings*.
34. S. Batsouli *et al.*, Phys. Lett. B 557 (2003) 26.
35. STAR TOF Collaboration, STAR TOF Proposal, 2004.
36. STAR HFT Collaboration, STAR HFT Proposal; K. Schweda *et al.* (STAR Collaboration), *these proceedings*.
37. A. Taketani *et al.* (PHENIX Vertex Group), *these proceedings*.